

Hierarchical Codebook-based Beam Training for Extremely Large-Scale Massive MIMO

Xu Shi, *Student Member, IEEE*, Jintao Wang, *Senior Member, IEEE*, Zhi Sun, *Senior Member, IEEE*, and Jian Song, *Fellow, IEEE*

Abstract—Extremely large-scale multiple-input multiple-output (XL-MIMO) promises to provide ultrahigh data rates in millimeter-wave (mmWave) and Terahertz (THz) spectrum. However, the spherical-wavefront wireless transmission caused by large aperture array presents huge challenges for channel state information (CSI) acquisition and beamforming. Two independent parameters (physical angles and transmission distance) should be simultaneously considered in XL-MIMO beamforming, which brings severe overhead consumption and beamforming degradation. To address this problem, we exploit the near-field channel characteristic and propose two low-overhead hierarchical beam training schemes for near-field XL-MIMO system. Firstly, we project near-field channel into spatial-angular domain and slope-intercept domain to capture detailed representations. Then we point out three critical criteria for XL-MIMO hierarchical beam training. Secondly, a novel spatial-chirp beam-aided codebook and corresponding hierarchical update policy are proposed. Thirdly, given the imperfect coverage and overlapping of spatial-chirp beams, we further design an enhanced hierarchical training codebook via manifold optimization and alternative minimization. Theoretical analyses and numerical simulations are also displayed to verify the superior performances on beamforming and training overhead.

Index Terms—XL-MIMO, beamforming design, hierarchical beam training, near-field, training overhead

I. INTRODUCTION

Massive Multiple-Input Multiple-Output (MIMO) is acknowledged as one of the key ingredients for the fifth generation (5G) of wireless communications, which has been standardized as 5G New Radio (NR) [1]–[4]. As the communication frequency-band is further extended to millimeter-wave (mmWave) and Terahertz (THz) spectrum, extremely large-scale massive MIMO (XL-MIMO) with significant number of antennas is promising to provide much stronger beamforming gain and higher spectrum efficiency [3]. However, caused by the large aperture arrays and corresponding high frequency band in XL-MIMO, Rayleigh distance may appear up to several hundred meters, which means the base station (BS) will serve large near-field (i.e., Fresnel region) areas inside Rayleigh distance [5], [6].

Specifically, spherical-wavefront assumption instead of conventional planar wavefront should be reconsidered in near-

This work was supported in part by Tsinghua University-China Mobile Research Institute Joint Innovation Center. (Corresponding author: Jintao Wang.)

Xu Shi, Jintao Wang, Zhi Sun, and Jian Song are with the Department of Electronic Engineering, Tsinghua University, Beijing 100084, China and Beijing National Research Center for Information Science and Technology (BNRist). (e-mail: shi-x19@mails.tsinghua.edu.cn).

field scenario. The corresponding channel is characterized by two independent parameters, i.e., the angle-of-departure/arrival (AoD/AoA) and transmission distance [7]. Under the specific near-field spherical-wavefront channel conditions, the transceiver, beamforming codebooks and CSI acquisition should be all redesigned for correct pair-matching of wireless channel. No matter whether analog or hybrid beamforming structures are adopted, conventional far-field beamforming codebook will suffer from deadly gain degradation and costly time complexity [8]. Moreover, the extremely large antennas and distance-sensitive channel steering response will herein bring about severe training overhead. Thus how to design the near-field beamforming codebook for XL-MIMO with low training overhead is urgent and significant.

A. Related works

The previous studies for near-field spherical-wavefront wireless electromagnetic radio transmission can be broadly separated into two categories: (a) One is sensing and localization of near-field sources [9]–[12]. Many maximum likelihood methods [11] and subspace-based methods were widely studied such as modified 2-dim multiple signal classification (2D-MUSIC) [10] and the spherical harmonics domain method [12]. Most methods in near-field localization and sensing involve large covariance matrix, higher-order statistics and multidimensional searching. Therefore, those methods are unsuitable for XL-MIMO beam training due to the huge computational complexity and overhead consumption. (b) The other related research direction is near-field sparse channel estimation via compressive sensing (CS) [8], [13], [14]. [13] uniformly divides the large aperture antenna array into several subarrays, and proposes a refined orthogonal matching pursuit (OMP)-based subarray/scatterer-wise channel estimation method. Furthermore, [8] exploits the polar-domain sparsity of near-filed XL-MIMO channel and designs a polar-domain simultaneous OMP algorithm for explicit CSI acquisition. However in CS-based estimation, the received signal-to-noise ratio (SNR) at user equipment (UE) side is usually quite low since the beamforming matrix needs random generation for restricted isometry property [15], which may cause CSI acquisition degradation. In another word, the implicit CSI acquisition, i.e., near-field beam training, is also significant, which seems more realistic and reliable for XL-MIMO.

Conventional far-field angular-domain beam training has been widely developed in both academic research and standardization progress. Hierarchical beam training is adopted

in IEEE 802.11ad/802.15.3c via sector level sweep (SLS), beam-refinement protocol (BRP) and beam tracking [16]. Besides, from an academic aspect, [17] utilized hierarchical weighted summation of sub-arrays and proposed a joint sub-array and de-activation (JOINT) hierarchical codebook. Enhanced JOINT (EJOINT) method was further proposed in [18] to avoid antenna de-activation. Furthermore, Riemannian optimization-based method [19] and successive closed-form (SCF) algorithm [20] were also adopted for efficient angular coverage and partition. However, notice that the near-field XL-MIMO beam training is completely different and seems more challenging. Given that additional distance dimension should be searched, more complicated codebook and corresponding hierarchical update policy should be further developed. And the overhead consumption and computational complexity also turn extremely demanding.

However, up to now, there exists limited research for near-field hierarchical beam searching. To our best knowledge, the only existing related work for XL-MIMO is [21], where the codewords are determined by a pair of uniformly sampled points in realistic space coordinate system. Hierarchical layers are controlled via different lengths of sampling spacing. This method is intuitive but not optimal unfortunately. The inter-beam interference and relevance are not thoroughly considered or analyzed in [21]. Consequently, nearby regions of BS may suffer from insufficient resolution due to its distance sensitivity while distance-insensitive far-field regions will be deployed with redundant codewords. In another word, the unfair distance-based codebook causes severe searching precision degradation and unnecessary training overhead. Furthermore, the codebook size will sharply boost as transmission distance raises, which is unacceptable for realistic communication.

B. Contributions

To summarize, the existing challenges in near-field XL-MIMO hierarchical beam training include: (1) how to overcome spatial non-stationarity and design elementary codebook to fully cover all possible beams; (2) how to generate several step-wise codebooks for hierarchical training to guarantee hierarchical searching success rate, and how to design the hierarchical update policy; (3) how to determine the hierarchical layer number, i.e., the theoretical analysis of minimal resolution and overhead consumption.

The main contributions of this paper are summarized as follows:

- We provide *joint spatial-angular* and *slope-intercept* representations for near-field spatial non-stationary channel. Inspired by Joint Time-Frequency Analysis (JTFA) and linear frequency modulation signal, we project the near-field beam steering vector into 2-dim spatial-angular plane and obtain its spatial non-stationary characteristic. Just like that far-field beam can be mapped into one point in 1-dim beamspace, we can project each near-field steering vector into one point at 2-dim slope-intercept domain. Thus overall uniformly quantized points in slope-intercept domain are collected into one group as the elementary codebook for XL-MIMO beam training.

- Based on the slope-intercept domain representation above, we further propose *three critical criteria* for XL-MIMO hierarchical beam training, which contains the requirement of codebook coverage, inter-codeword interference and generation complexity.
- Motivated by the characteristic of chirp signal, we propose one chirp-based hierarchical beam training scheme for near-field XL-MIMO and give the detailed hierarchical update policy. The spatial-chirp beam and its beam pattern in slope-intercept domain are fully exploited in the novel training scheme. Fortunately, the novel training method can approach high beamforming gain and sum-rate with quite low training overhead.
- Given the gap between ideal beam pattern and realistic spatial-chirp beam, we further propose an enhanced chirp-based hierarchical training scheme. Alternative minimization and Riemannian manifold optimization are adopted here to design the enhanced codebook. Through the enhanced scheme, the overlapping among spatial-chirp beams can be further eliminated and training success rate is significantly improved.
- Theoretical analyses of hierarchical layer number, beam training overhead and computational complexity are derived in this paper. Numerical results are provided to verify the effectiveness of chirp-based hierarchical training for near-field XL-MIMO. Training overhead can be reduced by over 97% without beamforming performance loss.

C. Organization and notations

The rest of this paper is organized as follows. In Section II, we introduce the XL-MIMO system and analyze near-field spherical-wavefront channel. In Section III, we give joint spatial-angular analysis of near-field channel and propose the slope-intercept domain representation of spatial non-stationary beams. The chirp-based hierarchical beam training scheme is proposed in Section IV, while we further design an enhanced scheme for overlapping elimination in Section V. Finally, we show the simulation results in Section VI and conclude this paper in Section VII.

Notations: Lower-case and upper-case boldface letters \mathbf{a} and \mathbf{A} denote a vector and a matrix respectively. \otimes and \circ denote the Kronecker product and Hadamard product, respectively. \mathbf{I}_M is identity matrix with size $M \times M$. The operator $\text{diag}(\mathbf{a})$ is a square diagonal matrix with entries of \mathbf{a} on its diagonal. The operators $\text{vec}(\cdot)$ and $\text{mat}(\cdot)$ denote the vectorizing of a matrix and matrix-reshape of a tensor, respectively. $\|\Delta\|_F$ and $\|\Delta\|_2$ denote Frobenius norm and l_2 norm for matrix Δ . $\mathcal{CN}(\mu, \Sigma)$ stands for a circularly symmetric complex Gaussian distribution with mean μ and variance Σ . $\text{rect}(2a)$ denotes a rectangular window with supporting interval $[-a, a]$ and $\angle \mathbf{a}$ denotes the element-wise phase extraction of vector \mathbf{a} .

II. SYSTEM MODEL

A. System and Problem Description

We consider a narrow-band downlink XL-MIMO system. Base station (BS) is configured with N_{BS} -element uniform

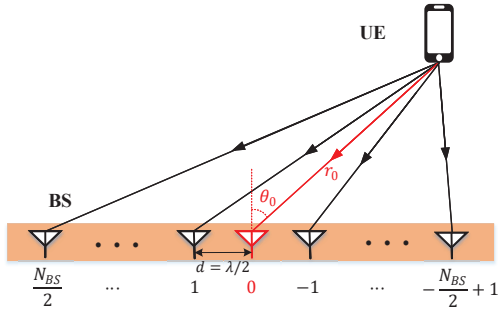


Fig. 1. Block diagram of near-field XL-MIMO system model.

linear array (ULA) with antenna indices as $n \in \{-\frac{N_{\text{BS}}}{2} + 1, \dots, \frac{N_{\text{BS}}}{2}\}$ ¹. Without loss of generality, we only consider one single-antenna user equipment (UE) as shown in Fig. 1. The distance and corresponding AoD between UE and BS array center (i.e., antenna element $n = 0$) are marked as r_0 and θ_0 ², respectively. The carrier frequency is set as f_c . Denote $d = \lambda/2$ as the fixed antenna spacing and $\lambda = c/f_c$ is the wavelength of electromagnetic waves. The overall ULA size is marked as $D = d(N_{\text{BS}} - 1) \approx dN_{\text{BS}}$. Therefore, the received noisy signal at UE can be formulated as

$$y_t = \mathbf{h}^T \mathbf{f}_t s_t + n_t, \quad (1)$$

where $\mathbf{f}_t \in \mathbb{C}^{N_{\text{BS}} \times 1}$ represents phase shifter (PS)-aided beam-forming vector in the t -th timeslot and $n_t \in \mathcal{CN}(0, \sigma_N^2)$ is additive white Gaussian noise (AWGN) with power σ_N^2 . \mathbf{h} denotes the Terahertz wireless channel and is written as

$$\mathbf{h} = \beta_{\text{LoS}} \mathbf{a}_{\text{LoS}} + \sum_{l=1}^{N_{\text{LoS}}} \beta_l \mathbf{a}_l, \quad (2)$$

β here is complex path loss and \mathbf{a} is the corresponding array steering vector with each entry $a_n = e^{-j2\pi r_n/\lambda}$. For LoS path, r_n denotes the distance between the n -th BS antenna and UE, while for NLoS path, r_n represents the distance between scatterer and n -th BS antenna.

The objective of beam training is to select the optimal codeword \mathbf{f}_{opt} from finite codebook \mathcal{F} to maximize the system spectral efficiency or beamforming gain. And the problem can be formulated as follows³:

$$\begin{aligned} \max_{\mathbf{f}} \quad & |\mathbf{h}^T \mathbf{f}|^2 \\ \text{s.t.} \quad & \mathbf{f} \in \mathcal{F} \quad \text{and} \quad |\mathbf{f}_n| = 1, \forall n \end{aligned} \quad (3)$$

Generally, the LoS path gain β_{LoS} is much larger than NLoS' gain β_l especially when carrier frequency is high enough such as mmWave and THz scenario, and thus in beam training we mainly focus on the strongest LoS beam searching.

¹UPA scenario can be similarly extended from ULA steering vectors by Kronecker product. We omit it here for brevity.

²In the following content, we only pay attention on AoD sine value and thus replace $\sin \theta_0$ with $\theta_0 \in [-1, 1]$ in array manifold for convenience.

³Multi-user scenario and multi-antenna UE scenario can be easily extended and we omit those for brevity. TDMA hierarchical beam training can support MU-XL-MIMO and in multi-antenna UE scenario, we could search codeword pairings at both BS and UE for the maximum beamforming gain.

B. XL-MIMO Channel Approximation

The main difference between XL-MIMO channel and conventional MIMO lies in the pattern of beam steering vector \mathbf{a}_{LoS} as follows. Since the carrier frequency f_c and antenna number turn extremely large, the Rayleigh length $r_R = \frac{2D^2}{\lambda}$ further increases and even gets larger than realistic supporting communication distance r_0 , which means that the far-field plane-wave assumption couldn't hold anymore. The transmission distance for n -th antenna element should be exactly calculated via cosine rule as:

$$\begin{aligned} r_n &= \sqrt{r_0^2 + (nd)^2 + 2r_0 nd \theta_0} \\ &\stackrel{(a)}{\approx} r_0 + \theta_0 \cdot nd + \frac{1 - \theta_0^2}{2r_0} \cdot (nd)^2, \end{aligned} \quad (4)$$

where (a) is approximated via Taylor Expansion, which has been widely adopted in previous near-field spherical-wave propagation model [5]. Notice that the first term is common to all antenna elements and is neglected here, the second term corresponds to conventional plane-wave array and the third term here is an additional component in spherical-wave XL-MIMO. Therefore the XL-MIMO array steering response $a_n = e^{-j2\pi r_n/\lambda}$ is approximate to

$$\begin{aligned} \hat{a}_n^{\text{n-f}} &= \exp \left\{ -j\pi \left(\theta_0 n + \frac{\lambda(1 - \theta_0^2)}{4r_0} n^2 \right) \right\} \\ &= \exp \left\{ -j\pi \left(\theta_0 + \frac{\lambda(1 - \theta_0^2)}{4r_0} n \right) \cdot n \right\} \end{aligned} \quad (5)$$

Correspondingly the near-field XL-MIMO beam training problem can be rewritten as

$$\begin{aligned} \max_{\mathbf{f}} \quad & |\hat{\mathbf{a}}_{\text{LoS}}^T \mathbf{f}|^2 \\ \text{s.t.} \quad & \mathbf{f} \in \mathcal{F} \quad \text{and} \quad |\mathbf{f}_n| = 1, \forall n \end{aligned} \quad (6)$$

Notice the problem here differs a bit from conventional MIMO system since the channel characteristic changes. Not only the AoD parameter but the distance-dependent second order term in (5) should be considered in the overall codebook design \mathcal{F} . Correspondingly, the beam training scheme and hierarchical update policy are also distinct. Herein, conventional far-field codebook will cause extreme beamforming degradation [18] while the previous distance-based near-field codebooks [21] cannot support accurate beam training due to the high pilot overhead and imperfect beam coverage. In this paper we mainly focus on the hierarchical beam training for XL-MIMO with joint consideration of *low overhead consumption, low computational complexity and perfect beam coverage*.

III. ELEMENTARY CODEBOOK DESIGN AND $k - l$ DOMAIN REPRESENTATION

Inspired by linear frequency modulation (LFM) signal $e^{-j\pi(f_0 + kt)t}$ (also named as chirp signal) in continuous wave radar, we can easily observe that the approximated near-field beam (5) has the same structure. The instantaneous AoA at each antenna element $\theta_n = \theta_0 + \frac{\lambda(1 - \theta_0^2)}{4r_0} n$ increases linearly with slope k and intercept b as:

$$k = \frac{\lambda(1 - \theta_0^2)}{4r_0}, \quad b = \theta_0. \quad (7)$$

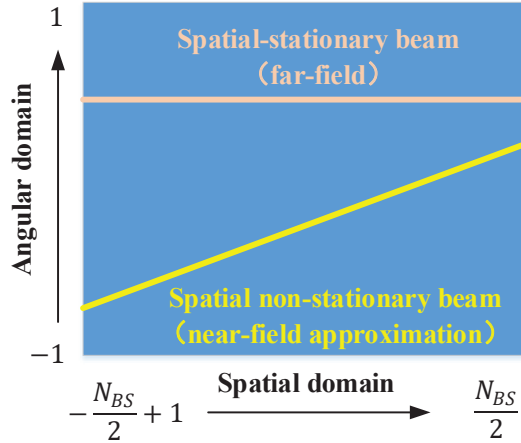


Fig. 2. Comparison of joint spatial-angular analysis for spatial stationary/non-stationary beam vectors.

However, it is worth noting that the near-field beam searching is quite different and much more challenging compared with LFM signal detection, this is because the spatial-sampling rate ($1/d$) and observation number (controlled by pilot length T) are both limited in beam searching. Thus conventional LFM detection schemes such as short-time Fourier transform (STFT) and ambiguity function cannot be adopted directly in XL-MIMO beam training. Compared with far-field antenna steering response $a_n^{f-f} = e^{-j\pi\theta_0 n}$ with $k = 0$, the near-field beam seems a classical spatial non-stationary signal. For more readability and easier analysis for channel characteristic, like Joint Time-Frequency Analysis (JTFA), we project the near/far-field beam vectors $\hat{\mathbf{a}}^{n-f} = [\hat{a}_n^{n-f}]$ and $\hat{\mathbf{a}}^{f-f} = [\hat{a}_n^{f-f}]$ into spatial-angular plane as shown in Fig. 2.

As for conventional far-field beam, since the overall beams' slope is fixed as 0, the searching of all AoA values (intercepts) is enough for the best beamforming direction selection. Furthermore, the conventional hierarchical searching is also intuitive: In the top hierarchical layers, wider beamforming vectors are equipped to coarsely search for a larger angular interval, and then in the next hierarchical layers the large interval is divided into several small fractions for more accurate beam training. In a word, the conventional codebooks can be easily generated by fully covering the angular domain $-1 \leq \theta_0 \leq 1$ with minimum beam interference.

On the contrary, in XL-MIMO model, we have to simultaneously estimate both the slope k and intercept b to determine the optimal spatial-chirp beam (5), which causes more pilot consumption and tremendous challenge in hierarchical codebook design. Different from previous studies that mainly focus on direction-distance-based codebook design, we herein decouple the two parameters and consider the direct quantization of k and b . Notice that the group (k, b) is equivalent to (θ_0, r_0) due to its injective property, but (k, b) is more general and low-complexity because of the decoupled relationship in chirp signal.

Then a trivial and elementary codebook can be generated by uniform quantization of k and b as shown in Fig. 3. First the intercept interval $[-1, 1]$ are uniformly quantized to N_{BS}

groups. Inside each quantized intercept b_q , several quantized slopes are independently modulated to form different chirp signals. The slope interval is marked as $[k_{\min}, k_{\max}]$ where $k_{\min} = 0$ corresponds to maximum transmission distance $r \rightarrow +\infty$ and $k_{\max} = \frac{\lambda}{4r_{\min}}$ corresponds to the minimum BS serve distance r_{\min} . The slope quantization spacing is defined as $\Delta k < k_{\text{TH}}$ and the threshold k_{TH} will be given in the following sections. Considering beams $\hat{\mathbf{a}}_1, \hat{\mathbf{a}}_2$ with common slope k and respective intercept θ_1 and $\theta_1 + p\frac{2}{N_{BS}}$ ($p \in \mathbb{Z}$), the beam coherence is strictly orthogonal as

$$g_b = |\hat{\mathbf{a}}_1^H \hat{\mathbf{a}}_2| = \sum_{n=1-N_{BS}/2}^{N_{BS}/2} e^{-j\pi p \frac{2}{N_{BS}} n} = N_{BS} \cdot \delta(p). \quad (8)$$

Considering beams $\hat{\mathbf{a}}_3, \hat{\mathbf{a}}_4$ with common intercept b and respective intercept $p\Delta k$ and $q\Delta k$ ($p, q \in \mathbb{Z}$), the beam coherence is derived as

$$g_k = |\hat{\mathbf{a}}_3^H \hat{\mathbf{a}}_4| = \sum_{n=1-N_{BS}/2}^{N_{BS}/2} e^{-j\pi(q-p)\Delta kn^2}. \quad (9)$$

which is a discrete Fresnel summation function with variable $(q - p)\Delta k$. Although the two beams here are not exactly orthogonal, we can control the coherence (interference) value via parameter design of Δk according to [8].

Next, we transform the spatial-angular domain into slope-intercept (k - b) plane as shown in Fig. 3. Each spatial-chirp beam (line in Fig. 3) is projected to one point with coordinate (k, b) and the whole codebook is just the uniform quantization of the 2-dim plane $[-1, 1] \times [k_{\min}, k_{\max}]$, defined as $\mathcal{F}_{\text{ele}} = \{\mathbf{w}_{k,b}\}$. A straightforward method to solve (6) in XL-MIMO is the exhaustive beam training, but we can obviously observe that the codebook size is quite huge and unacceptable for realistic traversal searching. For example, when $N_{BS} = 1024$, $f_c = 100\text{GHz}$ and $r_{\min} = 10\text{m}$, the corresponding codeword number is $1024 \times 16 = 16,384$. Therefore the hierarchical spatial-chirp beam training and corresponding codebook design scheme are necessary for low pilot consumption. Notice that the slope-intercept plane is the basis and kernel of the following content. Hierarchical codebook design, enhancement and the extension for other specific scenarios are all based on the k - b domain. Motivated by the idea in [18], we herein provide *three important criteria* for XL-MIMO hierarchical beam training as follows.

Criterion 1: The k - b domain regain union supporting by overall codewords in each hierarchical layer, should cover the whole k - b domain $[k_{\min}, k_{\max}] \times [-1, 1]$, i.e.,

$$\cup_{n=1}^{N^{(l)}} \left[\mathcal{R}(\mathbf{w}_n^{(l)}) \right] = [k_{\min}, k_{\max}] \times [-1, 1], l = 1, \dots, L. \quad (10)$$

where $\mathbf{w}_n^{(l)}$ represents the n -th codeword in the l -th hierarchical layer. $\mathcal{R}(\mathbf{w})$ denotes the beam coverage region in k - b domain and is mathematically expressed as

$$\mathcal{R}(\mathbf{w}) = \left\{ (k, b) \mid \mathbf{w} = \arg \max_{\mathbf{w}_n} |\mathbf{w}_n^H \mathbf{a}_{(k,b)}^{n-f}| \right\} \quad (11)$$

Criterion 2: The coverage region of any codeword $\mathbf{w}_n^{(l)}$, should be completely covered by the region union of several

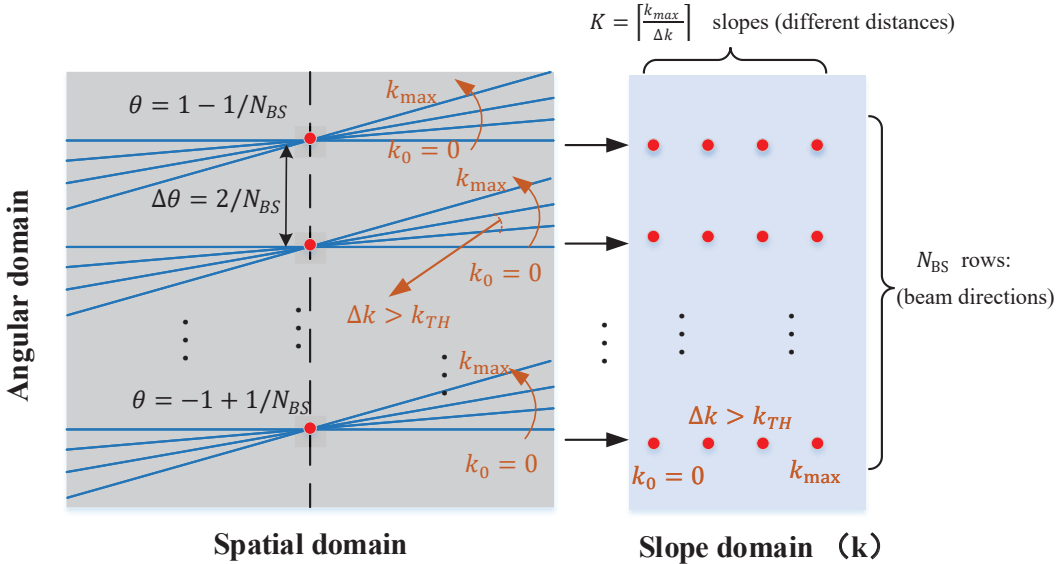


Fig. 3. Elementary codebook for near-field XL-MIMO in spatial-angular domain and slope-intercept (k - b) domain representation.

codewords in the next layer, i.e.,

$$\mathcal{R}(\mathbf{w}_n^{(l)}) \subseteq \cup_m \left[\mathcal{R}(\mathbf{w}_m^{(l+1)}) \right] \quad (12)$$

Criterion 3: Inside each layer, the rest codewords can be yielded from one codeword via beam rotation, which also means the dominant k - b domain regions for all codewords should contain the same size and geometric shape, i.e.,

$$\begin{aligned} \mathbf{w}_n^{(l)} &= \mathbf{w}_1^{(l)} \circ \mathbf{a}_{(p_n \Delta k, q_n \Delta b)}^{\text{n-f}} \\ \mathcal{R}(\mathbf{w}_n^{(l)}) &= \mathcal{R}(\mathbf{w}_1^{(l)}) + (p_n \Delta k, q_n \Delta b) \end{aligned} \quad (13)$$

To summarize, the above criterions aim to fully support and cover the overall k - b domain $[-1, 1] \times [k_{\min}, k_{\max}]$ with interference as small as possible. For the slope-intercept (k - b) domain, the following property can be easily yielded, which is helpful for the following derivations:

Theorem 1: Given any steering vector $\mathbf{v} \in \mathbb{C}^{N_{\text{BS}} \times 1}$ with unit-modulus entries ($|v_n| = 1$), for k_0 -th column's overall N_{BS} normalized codewords ($\mathbf{w}_{k_0, b}$ with all uniformly quantized $b \in [-1, 1]$ and fixed $k = k_0$, $\|\mathbf{w}_{k_0, b}\|_F^2 = 1$), the summation of coherence square is constant and equal to

$$\sum_{b_q} |\mathbf{w}_{k_0, b_q}^H \mathbf{v}|^2 = N_{\text{BS}}, \quad \forall k_0 \in [k_{\min}, k_{\max}] \quad (14)$$

Proof: For any column of k - b domain with $k = k_0$, the normalized codewords insides are formulated as

$$\mathbf{w}_{k_0, b_q} = \left[\frac{1}{\sqrt{N_{\text{BS}}}} \cdot e^{-j\pi(k_0 n^2 + b_q n)} \right], \quad (15)$$

and the coherence square summation is

$$\begin{aligned} \sum_{b_q} |\mathbf{w}_{k_0, b_q}^H \mathbf{v}|^2 &= \sum_{b_q} \left| \sum_n \left(\frac{1}{\sqrt{N_{\text{BS}}}} e^{-j\pi k_0 n^2} e^{-j\pi b_q n} v_n \right) \right|^2 \\ &= \sum_{b_q} \left| \frac{1}{\sqrt{N_{\text{BS}}}} \sum_n v'_n e^{-j\pi b_q n} \right|^2 \end{aligned} \quad (16)$$

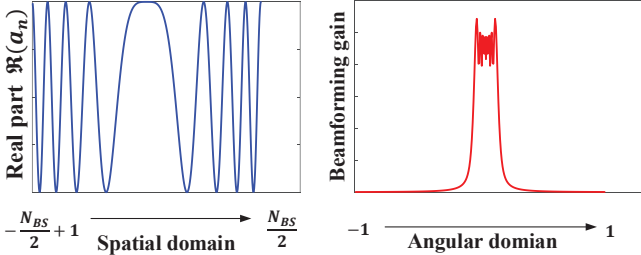
where $\mathbf{v}' = [v_n e^{-j\pi k_0 n^2}]$ is auxiliary vector. Notice the final result of (16) is just the overall power of \mathbf{v}' in frequency (angular) domain. According to Parseval's theorem [22], we can get that the power in frequency (angular) domain is equal to the power in time (spatial) domain. Since \mathbf{v}' is still with all entries unit-modulus ($|v'_n| = 1$), the time (spatial) domain power is $\mathbf{v}'^H \mathbf{v}' = N_{\text{BS}}$ and thus we finish the proof of Theorem 1.

Besides we can also obtain the same result via fractional Fourier Transform (FrFT) with different rotation angles. ■

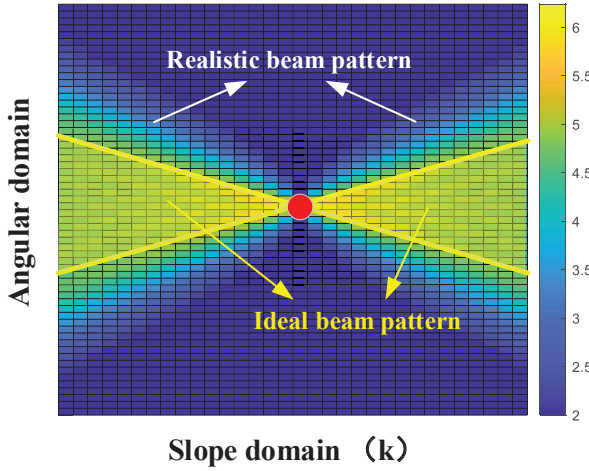
Remark 1: From Theorem 1 we get that: All beamforming codewords contain the same power N_{BS} when we project it into each column of k - b domain, which also means that, we cannot design such a simple codeword that only scans for a fraction in slope k axis. At least, it is quite difficult to find a beamforming vector that only supports a fractional square $[k_1, k_2] \times [b_1, b_2]$ (with the rest domain's coherence all zero) inside the whole domain $[k_{\min}, k_{\max}] \times [-1, 1]$. In another word, even if such codewords are designed, the corresponding inter-codeword interference and beam training overhead may further degenerate since the rest k - b region's power is not fully considered or exploited.

IV. CHIRP-BASED HIERARCHICAL BEAM TRAINING

In this section, we propose a chirp-based hierarchical codebook design scheme. Spatial-chirp signal's characteristics are fully analyzed and exploited to reduce redundant training



(a) Spatial-domain beam pattern and angular-domain beam pattern of near-field LoS channel.



(b) The ideal and realistic beam pattern of spatial-chirp beam in $k-b$ domain representation.

Fig. 4. The near-field LoS channel representation in spatial domain, angular domain and $k-b$ domain.

overhead. Corresponding hierarchical update policy and codeword distribution are designed here. Fortunately, the final training error probability, overhead consumption and average beamforming gain all get brilliant improvements through our proposed chirp-based hierarchical training scheme.

A. Spatial-Chirp Beam Pattern Analysis in $k-b$ Domain

As well known, chirp signal is a typical broadband signal, which is widely utilized for wideband target detection. To the best of our knowledge, in previous studies for far-field beam training, chirp signal (or quasi-chirp signal) has been adopted for hierarchical codebook design to scan for a large-size angular interval, like JOINT [17], EJOINT [18] and beam broadening [23]. This is because the broadband chirp signal can be conveniently controlled via only two parameters k and b , where k determines the beam width roughly while b controls the beam's central direction in far-field plane-wavefront assumption.

Therefore, we herein give an analysis for chirp signal first, which seems significantly useful for both far-field and near-field hierarchical beam training. According to Theorem 1, chirp beamforming signal also contains the same power along all columns' coherence. But the detailed coherence gain distribution inside $k-b$ domain is still not captured. Taking one spatial-chirp signal with $k = k_0$ and $b = b_0$ for example, the

mathematical expression $\mathbf{f}_{\text{eg}}(k_0, b_0)$ is written in (17), while the corresponding spatial-domain curve (real component) and angular-domain ($k=0$) curve (modulus) are shown in Fig. 4(a).

$$\mathbf{f}_{\text{eg}}(k_0, b_0) = \left[e^{-j\pi\left(k_0\left(-\frac{N_{\text{BS}}}{2}+1\right)^2+b_0\left(-\frac{N_{\text{BS}}}{2}+1\right)\right)}, \dots, 1, \dots, e^{-j\pi\left(k_0\left(\frac{N_{\text{BS}}}{2}\right)^2+b_0\frac{N_{\text{BS}}}{2}\right)} \right]^T \quad (17)$$

Following the results in LFM signals, when with large spatial-angular product $k_0 N_{\text{BS}}^2 \gg 1$ here, the angular bandwidth of the spatial-chirp signal $\mathbf{f}_{\text{eg}}(k_0, b_0)$ can be easily approximated to $B_0 = k_0 N_{\text{BS}}$, which also means that we can coarsely scan angular interval with length B_0 via $\mathbf{f}_{\text{eg}}(k_0, b_0)$. Similar to the proof in Theorem 1, we can further extend it to search for one column of $k-b$ domain with $k = k_1$, and the corresponding approximated searching angular bandwidth is derived as

$$B_{k_1} \approx |k_0 - k_1| N_{\text{BS}} \quad (18)$$

When $k_1 = k_0$, the scanning interval will degrade to one point, i.e., (k_0, b_0) in slope-intercept plane with power N_{BS} . Notice that each beam contains a bandwidth and thus the beam point (k_0, b_0) here also supports an intercept width as $\frac{2}{N_{\text{BS}}}$, which is consistent with unit bandwidth in orthogonal far-field discrete Fourier transform (DFT) codebooks [24]. Therefore, we coarsely approximate the bandwidth as $B_{k_1} \approx |k_0 - k_1| N_{\text{BS}} + \frac{2}{N_{\text{BS}}}$ for consistency. According to Theorem 1, the total power at each column $k = k_1$ is fixed as N_{BS} and corresponding interval length is B_{k_1} . Assume the power is uniformly distributed in the interval and thus the average gain (coherence) at each inside codeword point (b_q, k_1) can be yielded to N_{BS}/B_{k_1} , i.e.,

$$g_{b_q, k_1}^{\text{ideal}} = \begin{cases} \frac{N_{\text{BS}}}{B_{k_1}} \cdot \text{rect}\left(\frac{b_q - b_0}{B_{k_1}}\right) \\ \frac{1}{\sqrt{|k_0 - k_1| + 2/N_{\text{BS}}^2}}, \quad |b_q - b_0| \leq \frac{B_{k_1}}{2} \\ 0, \quad \text{else} \end{cases} \quad (19)$$

From above analysis we can get that, the ideal signal's searching range at k_1 column of $k-b$ plane is proportional to the distance $(|k_0 - k_1|)$ along k axis, while the ideal average gain at each point inside $k = k_1$ is approximately inversely proportional to the distance $|k_0 - k_1|$. Then we can depict this property into $k-b$ domain as shown in Fig. 4(b), where the darkness represents coherence amplitude between $\mathbf{f}_{\text{eg}}(k_0, b_0)$ and the corresponding local point. The specific coverage pattern is extremely instructive for the hierarchical codebook design in the 2-dim spatial-chirp beam training.

Remark 2: In this part, we only focus on the approximated interval-proportional distribution (i.e., the ideal beam pattern in Fig. 4(b)) to design each hierarchical layer's coarse coverage and training update policy. The realistic (standard) spatial-chirp signal instead of the ideal distribution is directly utilized for XL-MIMO beam training in the next subsection. Actually, the bandwidth approximation of chirp signal is not accurate when with small spatial-angular product $|k_0 - k_1| D^2 < \infty$. And then the realistic chirp signal will contain a roughly di-

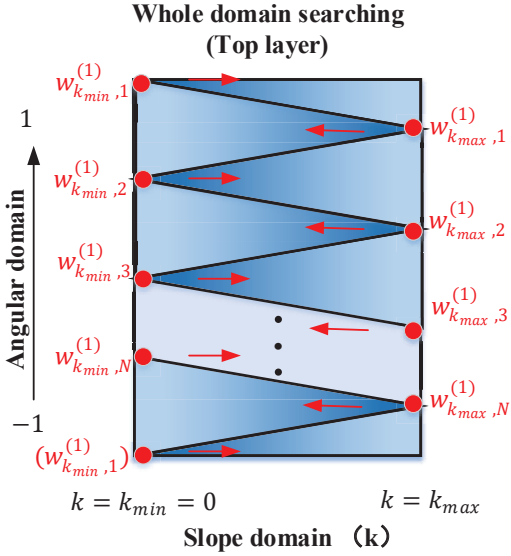


Fig. 5. Top-layer beam training codebook design for XL-MIMO.

vergent power distribution as shown in Fig. 4(b), which causes inter-chirp overlapping and higher searching error probability. For this reason principally, in Section V we further propose an enhanced codeword generation scheme for spatial-chirp beam modification and overlapping elimination.

B. Chirp-based Hierarchical Beam Training

1) Top layer hierarchical searching:

In the top-layer beam training, suppose the chirp-codewords are all selected at margin of $k-b$ domain $[k_{\min}, k_{\max}] \times [-1, 1]$. When the ideal beam pattern (18) (19) is assumed, to fully cover the whole $k-b$ domain, the corresponding chirp beam distribution should be designed as shown in Fig. 5. Each chirp beam can support beam searching inside a delta-shaped region. In Fig. 5 the darkness also denotes beamforming gain for the corresponding channel path with coordinate at each point. Define the i -th codeword at column k as $\mathbf{w}_{k,i}^{(1)}$, where index indicator $\ell = 1$ represents the top hierarchical layer. The angular sampling spacing and codeword number at top layer should follow the next theorem:

Theorem 2: In top-layer beam training, angular sampling spacing is at most $B_{\max} = \sqrt{2/N_{\text{BS}}}$ and thus the codeword number is at least $2\sqrt{2N_{\text{BS}}}$.

Proof: According to the near-field Fresnel region analysis [6], the distance lower bound of Fresnel region is $r_{\min} = 0.5\sqrt{\frac{D^3}{\lambda}}$. Therefore the minimum communication distance has $r_0 > r_{\min}$. Substituting it into (18) we can get that

$$B_{\max} = k_{\max}N_{\text{BS}} \leq \frac{\lambda}{4r_{\min}}N_{\text{BS}} = \sqrt{\frac{2}{N_{\text{BS}}}}. \quad (20)$$

In the top-layer searching, the codewords are all configured at two columns ($k = k_{\min} = 0$ and $k = k_{\max}$) with inter-column spacing B_{\max} , therefore we can obtain the total codeword

number at top hierarchical layer as

$$N^{(1)} = 2 \times \frac{1 - (-1)}{B_{\max}} = 2\sqrt{2N_{\text{BS}}}. \quad (21)$$

From Theorem 2 we can further write the coordinates of top-layer codewords as follows:

$$\begin{cases} \mathbf{w}_{k_{\min},i}^{(1)} : (k_{\min}, iB_{\max}); \\ \mathbf{w}_{k_{\max},i}^{(1)} : (k_{\max}, (i + 0.5)B_{\max}); \end{cases}, i = 1, \dots, N^{(1)} \quad (22)$$

This conclusion is quite succinct, which shows that the top-layer codeword number and supporting region only depend on the BS antenna number N_{BS} . For example, when we set carrier frequency $f_c = 30\text{GHz}$ and $N_{\text{BS}} = 512$, the minimum communication distance r_{\min} can be easily calculated as 8m. Thus the codeword number is obtained as $N^{(1)} = 20$, which seems acceptable for realistic beam training.

Besides, it is worth noting that wider region searching can also be similarly designed to further reduce training overhead. Instead of triangle-shape region, wider trapezoidal supporting region can be easily yielded when we further pull away and separate the two columns of codewords (For example, set codewords at columns $k = -k_{\max}$ and $k = 2k_{\max}$). Rectangle-shape region, i.e., the conventional far-field hierarchical training, can also be considered as one limit case for preliminary direction estimation.

2) Hierarchical Codeword Update Policy:

When the top-layer beam searching is addressed, we obtain the codeword with strongest beam gain which is herein marked as $\mathbf{w}_{\text{opt}}^{(1)}$. The corresponding $k-b$ domain triangle region is determined as $\mathcal{R}_{\text{opt}}^{(1)}$. Then we should allocate additional next-layer codewords for more accurate beam training and further reduce the potential beam region \mathcal{R}_{opt} until the region area satisfies highest resolution or approaches required beamforming gain.

As for each selected triangle region $\mathcal{R}_{\text{opt}}^{(1)}$, we divide it into four specific fractions, as shown in Layer 2 in Fig. 6(b). We'd like to discuss the problem in two cases. For Case 1 as shown in Fig. 6(b), the top-layer optimal region is a left triangle. Without loss of generality, we assume the optimal top-layer codeword is $\mathbf{w}_{\text{opt}}^{(1)} = \mathbf{w}_{k_{\min},2}^{(1)}$. Next in Layer 2, three additional codewords, i.e., $\mathbf{w}_1^{(2)}, \mathbf{w}_2^{(2)}$ and $\mathbf{w}_3^{(2)}$ are searched. The corresponding codewords' coordinates in $k-b$ domain can be easily obtained as middle points of the three sides of triangle $\mathcal{R}_{\text{opt}}^{(1)}$, i.e.,

$$\begin{cases} \mathbf{w}_1^{(2)} : \left(\frac{k_{\min} + k_{\max}}{2}, (i - 0.25)B_{\max} \right); \\ \mathbf{w}_2^{(2)} : \left(\frac{k_{\min} + k_{\max}}{2}, (i + 0.25)B_{\max} \right); \\ \mathbf{w}_3^{(2)} : (k_{\max}, iB_{\max}); \end{cases} \quad (23)$$

When in this example with $\mathbf{w}_{\text{opt}}^{(1)} = \mathbf{w}_{k_{\min},2}^{(1)}$, set $i = 2$ in (23) and the three codewords are then obtained. Notice that the temporary codeword subset $\{\mathbf{w}_{k_{\min},2}^{(1)}, \mathbf{w}_1^{(2)}, \mathbf{w}_2^{(2)}, \mathbf{w}_3^{(2)}\}$ can

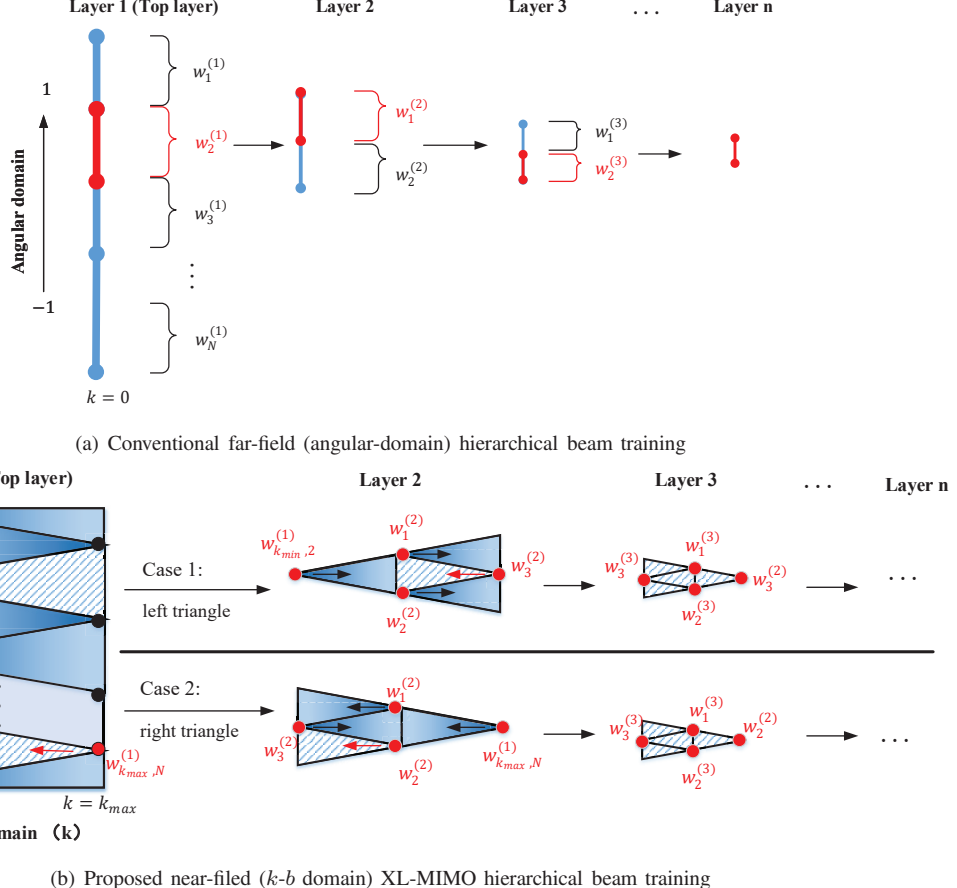


Fig. 6. The hierarchical beam training and codeword update rule for (a) conventional far-field (angular-domain) system model; (b) near-field (k - b domain) XL-MIMO system.

uniformly divide region $\mathcal{R}_{\text{opt}}^{(1)}$ into four non-overlapping sub-triangles and each codeword dominates in one sub-region, which means by comparing the four codewords' beamforming gains, we can further reduce the potential regain by four times. Both k dimension and b dimension can be reduced by half. By several 2-dim binary search, we can successively obtain $\mathcal{R}_{\text{opt}}^{(3)}$, \dots , $\mathcal{R}_{\text{opt}}^{(l)}$, \dots until l approaches the maximum hierarchical layer L and then get the final beam training result $\mathbf{w}_{\text{opt}}^{(L)}$. For the other case (Case 2: right triangle) in Fig. 6(b), we omit its detailed description for brevity since its process is quite similar to Case 1. The corresponding updated codewords' coordinates of Case 2 can be formulated as:

$$\begin{cases} \mathbf{w}_1^{(2)} : \left(\frac{k_{\min} + k_{\max}}{2}, (i - 0.25)B_{\max} \right); \\ \mathbf{w}_2^{(2)} : \left(\frac{k_{\min} + k_{\max}}{2}, (i + 0.25)B_{\max} \right); \\ \mathbf{w}_3^{(2)} : (k_{\min}, iB_{\min}); \end{cases} \quad (24)$$

In retrospect, the conventional far-field beam training can be regarded as a particular case of chirp-based XL-MIMO training. As shown in Fig. 6(a), if we only focus on the overall angular values with fixed slope $k = 0$, the 2-dim hierarchical searching procedure proposed above will degrade to angular

domain 1-dim hierarchical beam training, where two additional codewords are searched in each layer. From this point of view, our proposed near-field XL-MIMO hierarchical training contains only limited pilot overhead which is realistic and quite comparable to conventional mmWave binary hierarchical beam searching.

3) Quantization order calculation:

The next question is how to determine the value of maximum hierarchical layer L . Too large L is unnecessary due to redundant training overhead, while little L may cause training error and beamforming degradation. An intuitive idea is to first configure the angular quantization resolution as $2/N_{\text{BS}}$ (i.e. N_{BS} orthogonal DFT beam codewords for the whole angular domain, which is widely utilized). Since 2-dim binary search simultaneously processes on both intercept (b) domain and slope (k) domain, in a certain sense, the quantization of slope k is also determined. Therefore it is sufficient if we can prove that the above quantization of k is supportive and fully covers the whole slope interval $[0, k_{\max}]$.

From above analysis, the maximum angular bandwidth for top-layer codeword is $B_{\max} = k_{\max}N_{\text{BS}}$ while the slope-domain interval length is k_{\max} . When highest resolution of angular domain is set as $2/N_{\text{BS}}$, each top-layer codeword

contains

$$L_b^{(1)} = B_{\max} \sqrt{\frac{2}{N_{\text{BS}}}} = \frac{1}{2} k_{\max} N_{\text{BS}}^2 \quad (25)$$

basic quantized angular fractions and correspondingly the slope-domain fraction number is the same $L_k^{(1)} = L_b^{(1)}$. Therefore the basic slope-domain quantized fraction length can be calculated as

$$\Delta k = k_{\max} / L_k^{(1)} = \frac{2}{N_{\text{BS}}^2}. \quad (26)$$

According to the property of Fresnel integral and derivation in [8, Lemma 1], when the reciprocal of distance $1/r_0$ is uniformly quantized with quantization spacing smaller than threshold $\frac{2\lambda\beta^2}{N_{\text{BS}}^2 d^2 (1-\theta^2)}$, the beam can take a full coverage along slope domain. Substituting the threshold of quantized $1/r_0$ back to k (7) we can directly get the corresponding slope-domain quantization spacing as

$$k_{\text{TH}} = \Delta k^{\text{upper}} = \frac{2\lambda\beta^2}{N_{\text{BS}}^2 d^2 (1-\theta^2)} \cdot \frac{\lambda(1-\theta^2)}{4} = \frac{2\beta^2}{N_{\text{BS}}^2} \quad (27)$$

Compare the two spacing values Δk (26) and Δk^{upper} (27), and we can observe that the chirp-based slope quantization spacing can be designed from (27) with $\beta = 1$, and thus we have $\Delta k < \Delta k^{\text{upper}}$ since the upper-bounded β is approximately set as 1.6 in [8]. Therefore, we can confirm that Δk here is supportive for the whole slope interval $[0, k_{\max}]$.

To summarize, the whole hierarchical layer L can be calculated as

$$L = \left\lceil \log_2 \frac{1}{2} k_{\max} N_{\text{BS}}^2 \right\rceil. \quad (28)$$

Besides, when L is determined we can derive the top-layer codeword number as

$$N^{(1)} = 2 \times 2^{(\log_2 N_{\text{BS}} - L)} = 2^{1-L} N_{\text{BS}}. \quad (29)$$

Notice that this derivation (29) is consistent to (21) where we directly assume the minimum distance $r_0 = r_{\min} = 0.5 \sqrt{\frac{D^3}{\lambda}}$. And it is worth noting that the tradeoff appears when taking joint consideration of (28) and (29). If the minimum distance r_0 increases caused by environment variance, k_{\max} decreases and correspondingly, we need fewer hierarchical layers L but more codewords in top layer. The concrete steps of the proposed chirp-based hierarchical beam training scheme are displayed in Algorithm 1 as follows.

V. ENHANCEMENT OF CHIRP-BASED HIERARCHICAL CODEBOOK

A. Chirp-based Codeword Modification

In this subsection, we propose an enhanced hierarchical codebook design method for XL-MIMO system. Based on Principle of Stationary Phase (PSP) [25], the numerical solution of spatial-chirp signal's angular amplitude at $\theta = \theta_0$ can be approximately calculated as

$$G(\theta_0, \hat{\mathbf{a}}_{k,b}^{\text{n-f}}) = \frac{1}{\sqrt{2k}} \sqrt{[C(X_1) + C(X_2)]^2 + [S(X_1) + S(X_2)]^2} \quad (30)$$

where $C(X) = \int_0^X \cos(\frac{\pi x^2}{2}) dx$ and $S(X) = \int_0^X \sin(\frac{\pi x^2}{2}) dx$ are Fresnel integral, and the variables X_1 and X_2 are written

Algorithm 1 Proposed Chirp-based hierarchical beam training for near-field XL-MIMO

Input: System configurations N_{BS} , f_c , d and minimum communication distance d_{\min} , required beamforming gain threshold g_{th} .

Output: Beam training result \mathbf{b}

- 1: Calculate $k_{\max} = \frac{\lambda}{4r_{\min}}$, hierarchical layer L (28), top-layer codeword number $N^{(1)}$ (29) and angular-domain spacing $B_{\max} = k_{\max} N_{\text{BS}}$
%% Top-layer search
- 2: Generate top-layer codewords via (22) and search for the codeword with maximum beamforming gain $\mathbf{w}_{\max}^{(1)}$. Mark the corresponding k - b domain region as $\mathcal{R}_{\text{opt}}^{(1)}$.
%% Hierarchical search
- 3: **for** layer index $l = 2$ to L **do**
- 4: Divide region $\mathcal{R}_{\text{opt}}^{(i)}$ into four fractions and generate corresponding four dominant codewords in i -th layer $\{\mathbf{w}_{\max}^{(i-1)}, \mathbf{w}_1^{(i)}, \mathbf{w}_2^{(i)}, \mathbf{w}_3^{(i)}\}$ via (23) and (24)
- 5: Select the best codeword with maximum gain $\mathbf{w}_{\max}^{(i)}$ and update the optimal region $\mathcal{R}_{\text{opt}}^i$
- 6: **end for**
- 7: Final optimal supporting beam $\mathbf{b} \leftarrow \mathbf{w}_{\text{opt}}^{(L)}$

as follows. The results here are simple through POSP and thus we omit detailed derivation for brevity.

$$X_1 = \frac{kN_{\text{BS}} + (\theta_0 - b)}{\sqrt{2k}}, \quad X_2 = \frac{kN_{\text{BS}} - (\theta_0 - b)}{\sqrt{2k}}. \quad (31)$$

Actually as shown in (30), the realistic chirp signals could never keep standard triangle region like (18) and (19), and the bias is vividly compared in Fig. 4(b). Therefore, the overlapping among several chirp beam vectors may cause training error and thus degrade the following beamforming gain, which seems a challenging problem in the proposed chirp-based hierarchical training above.

To approach the ideal beam pattern (18) and (19) as much as possible, we establish a general optimization framework for each hierarchical layer, with initial input as spatial-chirp beam vectors. Notice that inside each layer we only need to design one codeword $\mathbf{w}_{\text{enh}}^{(l)}$ and the rest can be directly generated by shifting by $(p_n \Delta k, q_n \Delta b)$, so we only consider one fixed initial input chirp beam \mathbf{w}_0 : $(k, b) = (0, 0)$.

For the l -th layer, the total ideal dominant region $\hat{\mathcal{R}}_{\text{ideal}}^{(l)}$ contains two sub-regions, i.e., the combination of right triangle and left triangle. Since the dominant direction (right or left) is controlled by the $(l-1)$ -th layer's searching result, the two cases may both appear and thus we have to take joint consideration of the two directions. The corresponding triangle side (b -axis) $B_{\max}^{(l)}$ and height (k -axis) $k^{(l)}$ are yielded to

$$B_{\max}^{(l)} = k_{\max} N_{\text{BS}} 2^{1-l}, \quad k^{(l)} = k_{\max} 2^{1-l} \quad (32)$$

Following the chirp-based quantization order and codeword distribution in Algorithm 1, we can discretize the ideal region $\hat{\mathcal{R}}_{\text{ideal}}^{(l)}$ to several bottom-layer codewords. Inside l -th layer region $\hat{\mathcal{R}}_{\text{ideal}}^{(l)}$ there exist $2L_k^{(l)} - 1$ ($L_k^{(l)} = 2^{L-l+1}$) columns $k_p^{(l)} = p \Delta k$, $p = 1 - L_k^{(l)}, \dots, -1, 0, 1, \dots, L_k^{(l)} - 1$, and cor-

responding codeword numbers are $L_k^{(l)}, \dots, 2, 1, 2, \dots, L_k^{(l)}$, respectively. Therefore the ideal gain (coherence with quantized beam codeword $(k_p^{(l)}, b_q)$) for layer l is formulated as

$$G_l(k_p^{(l)}, b_q) = \begin{cases} \sqrt{\frac{N_{\text{BS}}}{|p|+1}}, & |b_q| \leq N_{\text{BS}}|k_p^{(l)}|, k_p^{(l)} = p\Delta k, \\ 0, & \text{else} \end{cases}$$

$$p = 1 - L_k^{(l)}, \dots, -1, 0, 1, \dots, L_k^{(l)} - 1 \quad (33)$$

Inside the l -th layer, the optimization objective is established as follows to reduce the gap between realistic beam vector and ideal beam pattern:

$$\begin{aligned} \min_{\mathbf{b}^{(l)}} \quad & \left\| \left(\mathbf{r}_l - |\mathbf{A}_l^H \mathbf{b}^{(l)}| \right) \circ \phi_l \right\|^2 \\ \text{s.t.} \quad & |\mathbf{b}^{(l)}(n)| = 1, \forall n = 1, \dots, N_{\text{BS}} \end{aligned} \quad (34)$$

where $\mathbf{A}_l = \text{mat}(\mathcal{A}_l)$, $\mathcal{A}_l \in \mathbb{C}^{N_{\text{BS}} \times N_{\text{BS}} \times (2L_k^{(l)}-1)}$ is the beam steering tensor with overall quantized beam vectors inside region $[-k^{(l)}, k^{(l)}] \times [-1, 1]$ into one group, and $\mathbf{r}_l = \text{vec}(\mathbf{G}_l)$, $\mathbf{G}_l = [G_l(k_q^{(l)}, b_q)] \in \mathbb{C}^{N_{\text{BS}} \times (2L_k^{(l)}-1)}$ denotes the perfectly ideal quantized coherence gain vector in this region. Besides, $\phi_l = \text{vec}(\Phi_l)$, $\Phi_l \in \mathbb{R}^{N_{\text{BS}} \times (2L_k^{(l)}-1)}$ is a fixed reweight matrix for l -th layer's codeword design. Generally, we can set $\Phi_l = \mathbf{1}_{N_{\text{BS}} \times (2L_k^{(l)}-1)}$ for equitable weights. On the other hand, notice that the overlapping among chirp-based codewords usually appears at two sides $k = \pm k^{(l)}$ as shown in Fig. 4(b). We tend to design the reweight matrix Φ_l with larger weights at two sides as follows

$$\Phi_l = [\underbrace{L_k^{(l)}, \dots, 3, 2, 1, 2, 3, \dots, L_k^{(l)}}_{2L_k^{(l)}-1 \text{ values}}] \otimes \mathbf{1}_{N_{\text{BS}} \times 1}. \quad (35)$$

By introducing an auxiliary phase vector $\psi^{(l)}$ the previous objective (34) is reformulated as

$$\begin{aligned} \min_{\mathbf{b}^{(l)}, \psi^{(l)}} \quad & \left\| \left(\mathbf{r}_l \circ e^{j\psi^{(l)}} - \mathbf{A}_l^H \mathbf{b}^{(l)} \right) \circ \phi_l \right\|^2 \\ \text{s.t.} \quad & |\mathbf{b}^{(l)}(n)| = 1, \forall n = 1, \dots, N_{\text{BS}} \end{aligned} \quad (36)$$

and then the problem can be easily solved by alternating minimization. With $\mathbf{b}^{(l)}$ fixed we can easily obtain the closed-form solution of $\psi^{(l)}$. When we fix $\psi^{(l)}$ to optimize codewords, we utilize manifold gradient optimization to deal with the non-convex constant-modulus constraint.

Firstly, with codeword vector $\mathbf{b}_t^{(l)}$ fixed where t denotes iteration index, the closed-form optimal solution of auxiliary phase vector $\psi_t^{(l)}$ is yielded to

$$\psi_t^{(l)} = \angle \mathbf{A}_l^H \mathbf{b}_t^{(l)} \quad (37)$$

Secondly, with phase vector $\psi_t^{(l)}$ fixed, we project the variable $\mathbf{b}^{(l)}$ into complex unit-circle Riemannian manifold [26] $\mathcal{M}_{\text{cc}}^{N_{\text{BS}}} = \{\mathbf{b} \in \mathbb{C}^{N_{\text{BS}} : |b(1)| = \dots = |b(N_{\text{BS}})| = 1}\}$. The tangent space at one point on the manifold $\mathbf{b} \in \mathcal{M}_{\text{cc}}^{N_{\text{BS}}}$ is

formulated as

$$T_{\mathbf{b}} \mathcal{M}_{\text{cc}}^{N_{\text{BS}}} = \{\mathbf{t} \in \mathbb{C}^{N_{\text{BS}}} : \mathbf{t}(n)\mathbf{b}(n)^* + \mathbf{t}(n)^*\mathbf{b}(n) = 0\}. \quad (38)$$

Then the corresponding Riemannian gradient $\text{grad}_{\mathcal{M}} f(\mathbf{b})$ is formulated as

$$\begin{aligned} \text{grad}_{\mathcal{M}} f(\mathbf{b}) &= \text{Proj}_{\mathbf{b}}(\nabla f(\mathbf{b})) \\ &= \nabla f(\mathbf{b}) - \Re(\nabla f(\mathbf{b}) \circ \mathbf{b}^*) \circ \mathbf{b}, \end{aligned} \quad (39)$$

and the corresponding Euclidean gradient of objective in (36) is given as

$$\nabla f(\mathbf{b}^{(l)}) = \mathbf{A}_l \left[\phi_l^2 \circ \left(\mathbf{A}_l^H \mathbf{b}^{(l)} - \mathbf{r}_l \circ e^{j\psi_t^{(l)}} \right) \right] \quad (40)$$

When we calculate gradient step size μ_t via Armijo rule [26], the codeword vector can be further updated:

$$\bar{\mathbf{b}}_t^{(l)} = \mathbf{b}_t^{(l)} - \mu_t \cdot \text{grad}_{\mathcal{M}} f(\mathbf{b}_t^{(l)}). \quad (41)$$

Notice that the temporary result $\bar{\mathbf{b}}_t^{(l)}$ doesn't satisfy the constant-modulus constraint, i.e., $\bar{\mathbf{b}}_t^{(l)} \notin \mathcal{M}_{\text{cc}}^{N_{\text{BS}}}$. Retraction procedure is necessary to fine-tune and map the temporary result on the tangent space to the complex circle manifold. According to [26], the retraction operator is utilized as follows

$$\begin{aligned} \mathbf{b}_{t+1}^{(l)} &= \text{Retr}_{\mathbf{b}_t^{(l)}} \left(\mu_t \cdot \text{grad}_{\mathcal{M}} f(\mathbf{b}_t^{(l)}) \right) \\ &= \text{vec} \left[\frac{\bar{\mathbf{b}}_t^{(l)}(n)}{|\bar{\mathbf{b}}_t^{(l)}(n)|} \right]. \end{aligned} \quad (42)$$

After several iterations ($t = 1, \dots, T$) we obtain the near-optimal beamforming vector $\mathbf{b}_{\text{opt}}^{(l)} = \mathbf{b}_T^{(l)}$ for XL-MIMO. Notice that in each hierarchical layer, we only consider one codeword with coordinate $(k, b) = (0, 0)$ and $\mathbf{b}_{\text{opt}}^{(l)}$ is just the enhancement for it. Therefore in the l -th layer, we can modulate the enhanced basis $\mathbf{b}_{\text{opt}}^{(l)}$ to overall chirp-based codewords and derive the final enhanced codebook via (23), (24) and $\mathbf{b}_{\text{opt}}^{(l)}$ as

$$\mathbf{w}_{\text{enh},i}^{(l)} = \mathbf{b}_{\text{opt}}^{(l)} \circ \mathbf{w}_i^{(l)} \quad (43)$$

The detailed procedure above is summarized in Algorithm 2, which can be regarded as one enhanced codebook design for near-field XL-MIMO system.

B. Fine-tune for the Realistic Communication

Limited by the realistic communication environment and BS equipment, there usually exists one minimum communication distance $r_0 \geq r_{\min} \geq 0.5\sqrt{\frac{D^3}{\lambda}}$ as above analysis. Notice that in Section III we assume that k and b are mutually independent to avoid additional complexity. Actually the slope is partially controlled by intercept. For example, when the AoA is fixed as $\theta_0 = \pm 1$, the transmission distance for each antenna element is $r_n = r_0 + nd$ and thus the steering vector is $[\mathbf{a}]_n = e^{-j\pi n}$, i.e., $k = 0$ always holds and coordinate (k, b) with $k \neq 0, b = \pm 1$ is impossible. Therefore we can further cut off the feasible k - b domain region to reduce training overhead in this scenario.

First, given the minimum transmission distance r_{\min} , we can derive and compress the accurate supportive region of k - b

Algorithm 2 Proposed enhanced codebook design for XL-MIMO hierarchical beam training

Input: Parameters in Alg 1, maximum iteration number T .

Output: Beam training result \mathbf{b}

%% Initialization

- 1: Generate overall chirp-based codewords in all hierarchical layers $\{\mathbf{w}_i^{(l)}, i = 1, 2, \dots\}, l = 1, \dots, L$. Set $\mathbf{b}_1^{(l)} = \mathbf{0}$, i.e., $(k, b) = (0, 0)$ and calculate ideal beam gain distribution \mathbf{r}_l and supporting matrix \mathbf{A}_l in (34).

%% Alternating Minimization

- 2: **for** hierarchical layer $l = 1$ to L **do**
- 3: **for** iter num $t = 1$ to T **do**
- 4: Update auxiliary phase vector $\psi_t^{(l)}$ via (37)
- 5: Update codeword vector $\mathbf{b}_{t+1}^{(l)}$ through manifold gradient optimization via (39), (40), (41), (42)
- 6: **end for**
- 7: Calculate the enhanced codebook $\{\mathbf{w}_{\text{enh},i}^{(l)}, i = 1, 2, \dots\}$ in the l -th hierarchical layer via (43)
- 8: **end for**
- 9: %% Hierarchical beam training for XL-MIMO
- 10: Utilize the enhanced codebook for hierarchical beam training following Algorithm 1 (Step 3, 4 and 5).
- 11: Final optimal supporting beam $\mathbf{b} \leftarrow \mathbf{w}_{\text{enh},\text{opt}}^{(L)}$

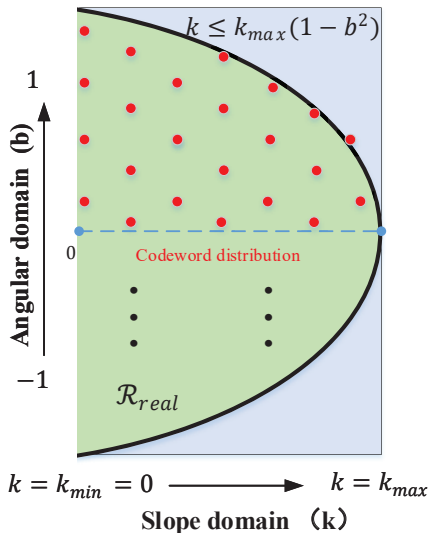


Fig. 7. Modified k - b domain codeword distribution for the realistic communication, where the minimum communication distance is preset.

domain with additional constraint (44) as shown in Fig. 7. The whole k - b region satisfying (44) is defined as $\mathcal{R}_{\text{real}}$.

$$k \leq \frac{\lambda}{4r_{\min}}(1 - b^2) \quad (44)$$

Next, for codebooks $\{\mathbf{w}_{\text{enh},i}^{(l)}\}$ in each hierarchical layer $l = 1, \dots, L$, we delete the codewords with all dominant region outsides ($\mathcal{R}_i^{(l)} \cap \mathcal{R}_{\text{real}} = \emptyset$) and only retain the rest codewords which contain sub-region inside constraint (44), i.e., the codewords with region intersection $\mathcal{R}_i^{(l)} \cap \mathcal{R}_{\text{real}} \neq \emptyset$. In this way, the codebook size can be further reduced for all hierarchical layers. Besides, the proposed hierarchical beam

training schemes for XL-MIMO is also promising and applicable in near-field RIS CSI acquisition, with joint consideration of previous estimation methods such as [27].

C. Performance Analysis

In this subsection we provide some performance evaluations about computational complexity of codebook generation and pilot consumption in hierarchical XL-MIMO beam training.

As for the pilot overhead consumption, at the top-layer there exist $2 \times \frac{N_{\text{BS}}}{L_k^{(1)}} = 2^{2-L} N_{\text{BS}}$ codewords for traversal search. And then at each layer from 2 to L , only four codewords are needed to fully cover the strongest beam in previous layer. Therefore, the overall pilot overhead number can be formulated as

$$P \leq 2^{2-L} N_{\text{BS}} + 4(L - 1). \quad (45)$$

and it is worth noting that the overhead at the top layer can be further reduced through beams with wider coverage. The corresponding beam pattern is slightly different but the codebook design and update rule are quite similar, as we described under (22). Even though we utilize the upper bound (45) for comparison, the excellent superiority still exists. For example, when we set carrier frequency $f_c = 50$ GHz, minimum communication distance $r_{\min} = 12$ m and $N_{\text{BS}} = 512$, we have $L = 5$ and corresponding pilot consumption is $P = 80$. As for conventional overall traversal search of k - b domain, the pilot consumption will increase to 8192. As for certain distance-based hierarchical training such as [21], assume the maximum transmission distance $r_{\max} = 1$ km and distance division spacing $\Delta r = 1$ m, overall 12516 pilots are even demanded to keep satisfying beamforming performance.

As for the computational complexity of enhanced codebook design, in each layer we only need to optimize one beamforming vector while other codewords can be directly obtained via beam rotation. The detailed complexity mainly lies in the matrix multiplications of manifold gradient optimization with $\mathcal{O}(TN_{\text{BS}}(2L_k^{(l)} - 1))$ and thus the overall computational complexity is yielded to

$$\mathcal{O} \left[\sum_{l=1}^L TN_{\text{BS}} (2L_k^{(l)} - 1) \right] = \mathcal{O} \left[TN_{\text{BS}} (2^L - 1 - L) \right]. \quad (46)$$

VI. SIMULATION RESULTS

In this section, numerical results are presented to verify the beamforming performance of our proposed chirp-based hierarchical beam training schemes.

In the simulation we assume that the central frequency is $f_c = 50$ GHz and BS antenna number is $N_{\text{BS}} = 512$. One single-antenna user is aligned to BS via beamforming for wireless communication. The LoS path gain obeys $\beta_{\text{LoS}} \sim \mathcal{CN}(0, 1)$ while the NLoS paths follow the i.i.d. Gaussian distribution $\beta_l \sim \mathcal{CN}(0, 10^{-3}), l = 1, 2, 3$. Based on the above configuration, we can easily calculate the minimum transmission distance $r_{\min} = 0.5 \sqrt{\frac{D^3}{\lambda}} = 12.29$ m. When the distance r_0 is not that large such as $r_0 \approx 40$ m, the near-field XL-MIMO channel characteristic dominates while when r_0 turns larger,

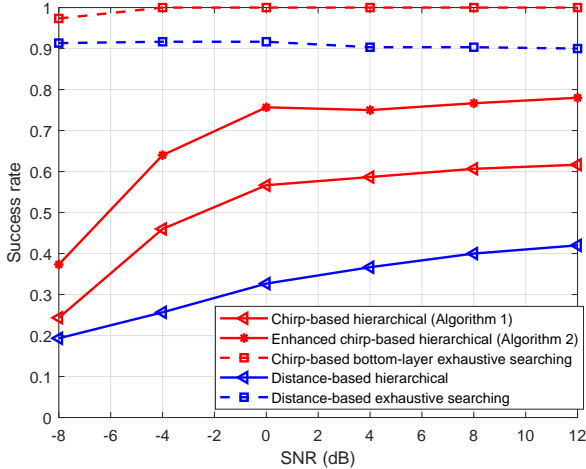


Fig. 8. Success rate of chirp-based and enhanced hierarchical searching schemes for near-field XL-MIMO, with $N_{\text{BS}} = 512$ and $f_c = 50$ GHz. Transmission distance r_0 and direction θ_0 are uniformly generated inside [13m, 100m] and $[-1, 1]$, respectively.

the conventional ray-based far-field channel characteristic will be dominant. Therefore, without loss of generality, we generate the transmission distance r_0 between BS array center and UE with uniform distribution $r_0 \sim \mathcal{U}([13\text{m}, 100\text{m}])$. Similarly, the relative direction θ_0 is uniformly generated inside the interval $[-1, 1]$. Then we can mathematically calculate the top-layer codeword number as $N^{(1)} = 64$ while the overall hierarchical layer number is $L = 5$.

As comparison, we herein simulate several other beam training schemes. Firstly, the beamforming scheme with perfect CSI is provided as the absolute upper bound. Besides, we collect and traverse the overall chirp-based bottom-layer codewords (exhausting searching without hierarchy) for CSI acquisition as a much tighter beamforming upper bound. Nevertheless, almost $N_{\text{BS}} \times 2^{L-1} = 8192$ overhead length is needed in traversal which is obviously unacceptable in realistic wireless communication. And the far-field codebook is also compared where we adopt and traverse the typical angular-orthogonal DFT codebook [24]. Since the far-field hierarchical searching obviously cannot achieve higher performance compared with traversal of DFT codebook, we neglect the simulation of conventional far-field (planar-wave) hierarchical searching such as JOINT or EJOINT. Besides, we also simulate near-field distance-based searching methods [21] where transmission distance are uniformly divided into several fractions for XL-MIMO codebook design.

Fig. 8 and Fig. 9 present the beam training success rate and communication sum-rate performances under different SNRs, respectively. The training success rate here is defined as follows. If the accurate LoS path information is captured, or the beamforming gain via hierarchical searching can approach 90% under perfect CSI, we regard the hierarchical scheme works successfully. In Fig. 8 and Fig. 9 we can observe that the elementary codebook (overall bottom-layer codewords) works well up to 100% success rate, which demonstrates the superiority of our proposed codewords. Nevertheless, the

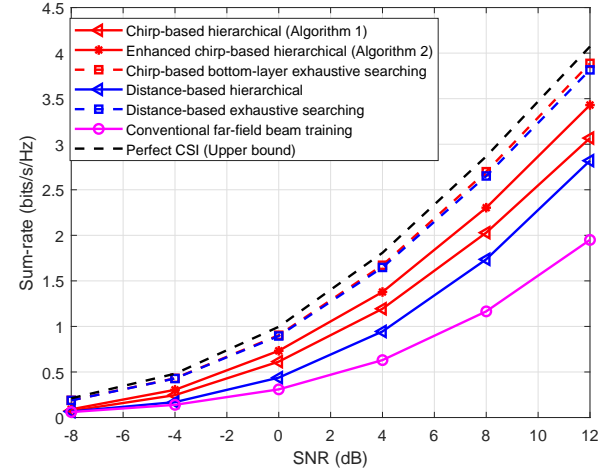


Fig. 9. Comparisons of average sum-rate against SNR for several hierarchical searching schemes in near-field XL-MIMO, with $N_{\text{BS}} = 512$ and $f_c = 50$ GHz.

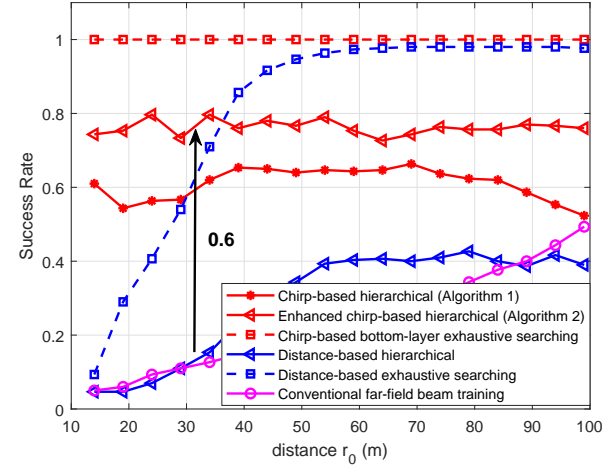


Fig. 10. Success rate of chirp-based and enhanced hierarchical searching schemes for near-field XL-MIMO, with SNR = 10 dB, $N_{\text{BS}} = 512$ and $f_c = 50$ GHz. Transmission direction θ_0 is uniformly generated inside $[-1, 1]$.

hierarchical searching couldn't obtain absolutely 100% success rate since there still exist overlapping and interference among hierarchical codewords. In fact, the ideal beam pattern \mathbf{G}_l in (33) is non-existent in practice and our proposed two hierarchical codebooks are just certain approximations of it. The mistakes are unavoidable during near-field hierarchical searching process. Thankfully, the success rate can be obviously improved via enhancement (Algorithm 2) compared with the initial chirp-based scheme (Algorithm 1), and the average sum-rate is supportive and outperforms conventional far-field training by almost 1.5 bits/s/Hz. And our proposed hierarchical schemes outperform distance-based training method [21] by over 0.7 bits/s/Hz.

The impacts of transmission distance are shown in Fig. 10 and Fig. 11, where we fix SNR as 10 dB. As shown here, the proposed chirp-based hierarchical training and enhanced hierarchical searching are both distance-insensitive. In another

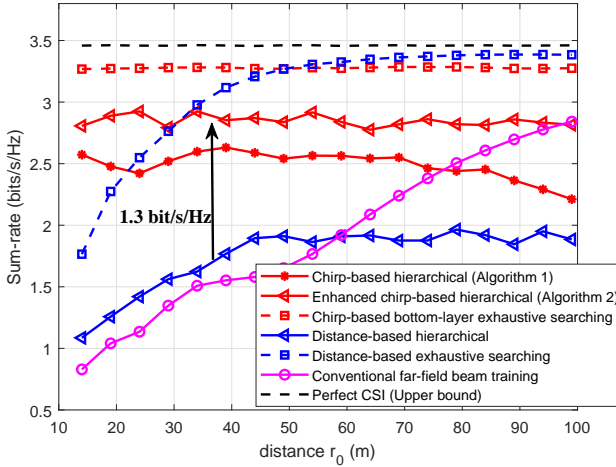


Fig. 11. Comparisons of average sum-rate against transmission distance for several hierarchical searching schemes in near-field XL-MIMO, with SNR = 10 dB, $N_{\text{BS}} = 512$ and $f_c = 50$ GHz.

word, the proposed two hierarchical training schemes can support both far-field and near-field scenarios with high sum-rate and beamforming gain, while the conventional DFT codebook can only provide strong support when $r_0 > 100$ m. In near-field scenario such as $r_0 = 30$ m, the DFT codebook can only approach sum-rate 1.5 bits/s/Hz but the proposed schemes outperform it by almost two times. And it is worth noting that, the enhanced chirp-based hierarchical scheme shows whole-distance superior performance which seems promising to replace conventional far-field training [24] or distance-based hierarchical searching [21] for higher communication robustness. Besides, the fluctuation of chirp-based training with distance r_0 (red curves) is normal since the transmission distance is non-linear quantized in the near-field hierarchical codebook, while the noise and residual overlapping among codewords also affect the success rate and curve fluctuation.

Next, we provide the beamforming gain during each hierarchical layer in Fig. 12. At the beginning (first three layers), initial chirp-based scheme obtains quite comparable beamforming gain to the enhanced scheme. And then in the next two bottom layers, the gap gets large to 6.25%. Compared with conventional DFT codebook, the average beamforming gain is further improved by 60% improvement. Frankly speaking, from beamforming gain perspective, there still exists a large gap between the enhanced chirp-based hierarchical scheme and exhaustive searching method and we take potential further optimization into future work.

Last but most important, we elaborate the pilot overhead consumption under different BS antenna configurations in Fig. 13. Compared with the bottom-layer overall codewords exhaustive searching, the overhead consumption can be reduced by over 99.5%, and over 97% overhead can be saved compared with distance-based hierarchical searching method [21]. For example, when the antenna $N_{\text{BS}} = 512$, the exhaustive searching needs overhead of about 8192, while the enhanced chirp-based hierarchical scheme only needs $2^{2-L}N_{\text{BS}} + 4(L-1) = 80$ overhead. Besides, the initial

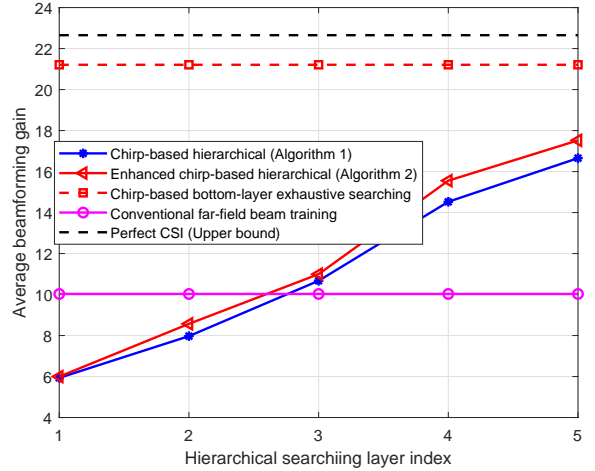


Fig. 12. Average beamforming gain during each search step (each layer) for several hierarchical beam training schemes.

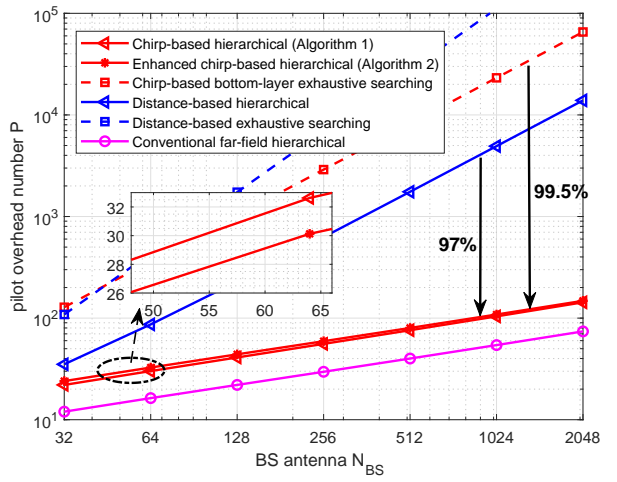


Fig. 13. Overall overhead consumption against BS antenna number.

chirp-based scheme (Algorithm 1) can further reduce the overhead consumption to $2^{2-L}N_{\text{BS}} + 3(L-1) = 76$, this is because in all hierarchical layers it utilizes the same standard spatial-chirp beams with different coordinates and the optimal codeword $\mathbf{w}_{\text{opt}}^{(l)}$ in layer l is reused in the next $(l+1)$ -th layer. Besides, it is worth noting that the main overhead consumption is from the top-layer searching where 64 overhead is allocated here and it can be further reduced through beams with wider trapezoidal coverage above top-layer searching. If the far-field hierarchical searching starts with the same angular resolution B_{max} (20), the total overhead can be calculated as $2^{1-L}N_{\text{BS}} + 2(L-1) = 40$. Therefore, we can conclude that compared with conventional DFT codebook and corresponding hierarchical schemes, our proposed near-field hierarchical searching for XL-MIMO can approach much more superior and robust performance with quite comparable overhead consumption.

VII. CONCLUSION

In this paper, we propose two low-overhead hierarchical beam training schemes for near-field XL-MIMO system to rapidly capture CSI with low training overhead consumption. Firstly, spatial-angular domain representation and slope-intercept domain representation are proposed to describe near-field channel. Based on the slope-intercept domain representation, we point out three critical criteria for XL-MIMO hierarchical beam training. Then inspired by the LFM Radar waveform, a novel spatial-chirp beam-aided codebook and corresponding hierarchical update policy are proposed. Furthermore, given the imperfect coverage and overlapping of spatial-chirp beams, we further design an enhanced hierarchical training codebook via manifold optimization and alternative minimization. Thankfully, the simulation results showed that the proposed two hierarchical searching schemes both have remarkable beam training performance with quite low overhead consumption.

REFERENCES

- [1] E. Björnson, L. Sanguinetti, H. Wymeersch, J. Hoydis, and T. L. Marzetta, "Massive mimo is a reality—what is next?: Five promising research directions for antenna arrays," *Digital Signal Processing*, vol. 94, pp. 3–20, 2019.
- [2] Z. Zhou, X. Gao, J. Fang, and Z. Chen, "Spherical wave channel and analysis for large linear array in los conditions," in *2015 IEEE Globecom Workshops (GC Wkshps)*, pp. 1–6, IEEE, 2015.
- [3] S. Hu, F. Rusek, and O. Edfors, "Beyond massive mimo: The potential of data transmission with large intelligent surfaces," *IEEE Transactions on Signal Processing*, vol. 66, no. 10, pp. 2746–2758, 2018.
- [4] B. Ning, Z. Tian, Z. Chen, C. Han, J. Yuan, and S. Li, "Prospective beamforming technologies for ultra-massive mimo in terahertz communications: A tutorial," *arXiv preprint arXiv:2107.03032*, 2021.
- [5] W. Southwell, "Validity of the fresnel approximation in the near field," *JOSA*, vol. 71, no. 1, pp. 7–14, 1981.
- [6] K. T. Selvan and R. Janaswamy, "Fraunhofer and fresnel distances: Unified derivation for aperture antennas," *IEEE Antennas and Propagation Magazine*, vol. 59, no. 4, pp. 12–15, 2017.
- [7] A. Swindlehurst and T. Kailath, "Passive direction-of-arrival and range estimation for near-field sources," in *IEEE Spec. Est. and Mod. Workshop*, vol. 123, Citeseer, 1988.
- [8] M. Cui and L. Dai, "Channel estimation for extremely large-scale mimo: Far-field or near-field?," *IEEE Transactions on Communications*, vol. 70, no. 4, pp. 2663–2677, 2022.
- [9] W. Zuo, J. Xin, N. Zheng, H. Ohmori, and A. Sano, "Subspace-based near-field source localization in unknown spatially nonuniform noise environment," *IEEE Transactions on Signal Processing*, vol. 68, pp. 4713–4726, 2020.
- [10] Y.-D. Huang and M. Barkat, "Near-field multiple source localization by passive sensor array," *IEEE Transactions on antennas and propagation*, vol. 39, no. 7, pp. 968–975, 1991.
- [11] J. C. Chen, R. E. Hudson, and K. Yao, "Maximum-likelihood source localization and unknown sensor location estimation for wideband signals in the near-field," *IEEE transactions on Signal Processing*, vol. 50, no. 8, pp. 1843–1854, 2002.
- [12] L. Kumar and R. M. Hegde, "Near-field acoustic source localization and beamforming in spherical harmonics domain," *IEEE Transactions on Signal Processing*, vol. 64, no. 13, pp. 3351–3361, 2016.
- [13] Y. Han, S. Jin, C.-K. Wen, and X. Ma, "Channel estimation for extremely large-scale massive mimo systems," *IEEE Wireless Communications Letters*, vol. 9, no. 5, pp. 633–637, 2020.
- [14] N. J. Myers, Y. Aslan, and G. Joseph, "Near-field focusing using phased arrays with dynamic polarization control," *arXiv preprint arXiv:2205.10243*, 2022.
- [15] C.-R. Tsai, Y.-H. Liu, and A.-Y. Wu, "Efficient compressive channel estimation for millimeter-wave large-scale antenna systems," *IEEE Transactions on Signal Processing*, vol. 66, no. 9, pp. 2414–2428, 2018.
- [16] J. Wang, Z. Lan, C. woo Pyo, T. Baykas, C. sean Sum, M. Rahman, J. Gao, R. Funada, F. Kojima, H. Harada, and S. Kato, "Beam codebook based beamforming protocol for multi-gbps millimeter-wave wpan systems," *IEEE Journal on Selected Areas in Communications*, vol. 27, no. 8, pp. 1390–1399, 2009.
- [17] Z. Xiao, T. He, P. Xia, and X.-G. Xia, "Hierarchical codebook design for beamforming training in millimeter-wave communication," *IEEE Transactions on Wireless Communications*, vol. 15, no. 5, pp. 3380–3392, 2016.
- [18] Z. Xiao, H. Dong, L. Bai, P. Xia, and X.-G. Xia, "Enhanced channel estimation and codebook design for millimeter-wave communication," *IEEE Transactions on Vehicular Technology*, vol. 67, no. 10, pp. 9393–9405, 2018.
- [19] W. Fan, C. Zhang, and Y. Huang, "Flat beam design for massive mimo systems via riemannian optimization," *IEEE Wireless Communications Letters*, vol. 8, no. 1, pp. 301–304, 2018.
- [20] O. Aldayel, V. Monga, and M. Rangaswamy, "Tractable transmit mimo beampattern design under a constant modulus constraint," *IEEE Transactions on Signal Processing*, vol. 65, no. 10, pp. 2588–2599, 2017.
- [21] X. Wei, L. Dai, Y. Zhao, G. Yu, and X. Duan, "Codebook design and beam training for extremely large-scale ris: Far-field or near-field?," *arXiv preprint arXiv:2109.10143*, 2021.
- [22] D. Tse and P. Viswanath, *Fundamentals of wireless communication*. Cambridge university press, 2005.
- [23] F. Gao, B. Wang, C. Xing, J. An, and G. Y. Li, "Wideband beamforming for hybrid massive mimo terahertz communications," *IEEE Journal on Selected Areas in Communications*, vol. 39, no. 6, pp. 1725–1740, 2021.
- [24] M. Xiao, S. Mumtaz, Y. Huang, L. Dai, Y. Li, M. Matthaiou, G. K. Karagiannidis, E. Björnson, K. Yang, I. Chih-Lin, et al., "Millimeter wave communications for future mobile networks," *IEEE Journal on Selected Areas in Communications*, vol. 35, no. 9, pp. 1909–1935, 2017.
- [25] R. Wong, *Asymptotic approximations of integrals*. SIAM, 2001.
- [26] P.-A. Absil, R. Mahony, and R. Sepulchre, *Optimization algorithms on matrix manifolds*. Princeton University Press, 2009.
- [27] X. Shi, J. Wang, and J. Song, "Triple-structured compressive sensing-based channel estimation for ris-aided mu-mimo systems," *IEEE Transactions on Wireless Communications*, pp. 1–1, 2022.